Activation of Hemolysin Toxin: Relationship between Two Internal Protein Sites of Acylation†

Keisha G. Langston, Lesa M. S. Worsham, Laurie Earls,‡ and M. Lou Ernst-Fonberg*

Department of Biochemistry and Molecular Biology, James H. Quillen College of Medicine, East Tennessee State University, Johnson City, Tennessee 37614

Received October 28, 2003; Revised Manuscript Received February 16, 2004

ABSTRACT: HlyC, hemolysin-activating lysine acyltransferase, catalyzes the acylation (from acyl-ACP) of *Escherichia coli* prohemolysin (proHlyA) on the ϵ-amino groups of specific lysine residues, Lys564 and Lys690 of the 1024-amino acid primary structure, to form hemolysin (HlyA). The amino acid sequences flanking the two acylation sites are not homologous except that each has a glycine residue immediately preceding the lysine which is acylated; there are, however, numerous GK sequences throughout proHlyA that are not acylation sites. The substrate specificity of acylation was examined. ProHlyA-derived structures, altered by substantial deletions and separation of the acylation sites into two different peptides and site-directed mutation analyses of acylation sites, often served as internal protein acylation substrates, and the kinetics of the acylations were measured. The two sites of acylation of proHlyA functioned independently of one another with HlyC; there did not appear to be a common HlyC binding site or processivity of the enzyme between the sites. Acyl-HlyC was likely the enzyme form that interacted with the final acylation substrate. In a variety of constructs, the two acylation sites had similar K_m values, but their V_{max} values and catalytic efficiencies as substrates differed. Internal protein acylation was inhibited by specific small peptides mimicking the primary structure of each acylation site except that the crucial lysines were replaced with arginines; similar small peptides containing the crucial lysine, however, were not acylated.

Fatty acylation of a protein is a means of modifying its biological behavior, sometimes reversibly. For example, the covalent attachment of fatty acids appears to be important in guiding subcellular trafficking of proteins. In this vein, fatty acylation is proposed to be a way of targeting proteins to membrane lipid rafts for subsequent signal transduction; notably, comparably hydrophobic prenyl groups do not substitute in this role for fatty acyl groups (*1*, *2*). Long chain fatty acylation of proteins to create acyl-proteins is achieved by diverse mechanisms. One class of acyl-proteins arises from cotranslational modification by amide linkage of myristic acid to their N-terminal glycine residues (*3*). In another, acylation occurs post-translationally on internal cysteine, threonine, or lysine residues, generating S- or O-esters or an amide, respectively (*4*, *5*); compared to N-terminal acylation, these processes are biochemically less understood. Numerous instances of protein internal fatty acylation, generally via thiol esterification of cysteine residues, have been noted (*6*), and palmitoylation of eukaryotic proteins has recently been examined with a view of its reversibility, i.e., phosphorylation and dephosphorylation (*7*). The extent of internal fatty acylation via amide linkage of mammalian proteins is unknown. Acylation of cellular proteins with endogenously synthesized fatty acids in a mouse muscle cell line suggested, however, that at least 30% of protein-bound palmitate was present in an amide linkage with undefined residues (*8*).

HlyC,[1] the hemolysin-activating lysine acyltransferase, is the only internal protein acyltransferase that has been biochemically examined; it catalyzes the internal acylation of *Escherichia coli* prohemolysin (proHlyA) with two fatty acyl groups to form hemolysin (HlyA) (*9*). This reaction is remarkable in that lipid modification changes the behavior of a protein from a benign protein to a toxin. Hemolysin is the prototype of the homologous RTX family of toxins secreted by Gram-negative bacteria; they are a biologically and economically important group of protein toxins that have a common operon structure and similar repetitive sequence motifs within the toxin. The varied host and cell specificities of the various RTX toxins are striking but unexplained (*10*). RTX toxins arise from the *A gene* of a *CABD* operon where

† This work was supported by National Institutes of Health Grant R01-GM62121.

* To whom correspondence should be addressed: Department of Biochemistry and Molecular Biology, James H. Quillen College of Medicine, Box 70581, East Tennessee State University, Johnson City, TN 37614. Phone: (423) 439-2025. Fax: (423) 439-2030. E-mail: ernstfon@mail.etsu.edu.

‡ Present address: Department of Pharmacology, Vanderbilt University, 446 Robinson Research Building, Nashville, TN 37232.

[1] Abbreviations: proHlyA, *E. coli* hemolysin A protoxin; HlyA, *E. coli* hemolysin A toxin; RTX, repeats in toxin; HlyC, hemolysin-activating lysine acyltransferase, an acyl-ACP-proHlyA acyltransferase; CyaA, *B. pertussis* RTX toxin; ACP, acyl carrier protein; ACPSH, acyl carrier protein with a free prosthetic group thiol; myristoyl-ACP, acyl carrier protein with a 14-carbon acyl chain covalently attached to the prosthetic group thiol; acyl-ACP, acyl carrier protein with a long chain fatty acyl covalently attached to the prosthetic group thiol; Hepes, *N*-(2-hydroxyethyl)piperazine-*N*′-2-ethanesulfonic acid; EDTA, ethylenediaminetetraacetic acid; IPTG, isopropyl β-D-thiogalactopyranoside; SDS, sodium dodecyl sulfate; PAGE, polyacrylamide gel electrophoresis; PCR, polymerase chain reaction; ND, not determined.

10.1021/bi035919k CCC: $27.50
Published on Web 03/19/2004

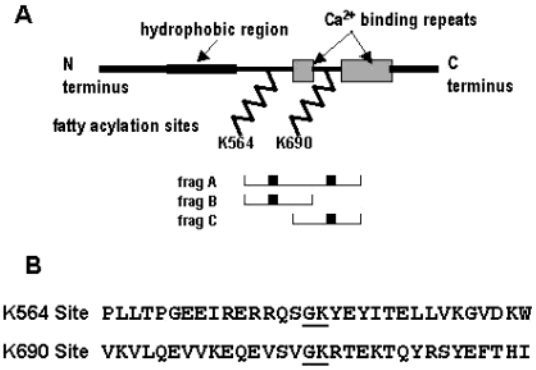

FIGURE 1: Hemolysin structure scheme and amino acid residues surrounding the acylation sites. (A) Diagram of the hemolysin structure and fragments of it showing the two acylation sites, Lys564 and Lys690. (B) Amino acid residues surrounding the two underlined acylation sites.

the *C gene* product is the acyltransferase that transfers acyl groups to the A protein. Acyl-ACP is the obligate acyl donor in *E. coli* (*11*, *12*), where HlyA is acylated on the ϵ-amino groups of lysine residues 564 and 690 of the 1024-amino acid primary structure (*13*). Most other RTX toxins are likely homologously acylated. The identities and functional specificities, if any, of the acyl groups are unresolved in most instances. In vivo acylation of *E. coli* HlyA results in heterogeneous, diacyl, covalent structures containing saturated fatty acyl groups of 14-carbon (68%), 15-carbon (26%), and 17-carbon (6%) amide-linked side chains, while in comparison, the acylations observed in RTX toxin from *Bordetella pertussis* (CyaA) are highly variable (*14*).

Although binding to membranes can occur without acylation, the biological activity of hemolysin toxin requires acylation (*15*−*17*). The toxic action of HlyA is not restricted to cell lysis; it entrains more subtle but consequential manifestations in infected cells. HlyA's function in pyelonephritis was recently unequivocally shown, and bacterial lipopolysaccharide and proHlyA have no effect or contribution (*18*). HlyA alone interacting appropriately with the plasma membrane acts as an inducer of an oscillating second messenger response in target primary rat renal epithelial cells, resulting in a constant, low-frequency oscillatory Ca^{2+} response that stimulates production of cytokines interleukin-6 and interleukin-8. The launch of biologic events by sublytic concentrations of HlyA resulting in induction of a second messenger response in host cells that, in turn, results in the induction of inflammation and probably other unidentified cellular events shows the dramatic consequences of the internal acylation of a protein.

Using separately subcloned, expressed, and purified proteins participating in the internal acylation of proHlyA to form HlyA, we have previously characterized the acyltransferase HlyC and the reaction it catalyses, the transfer of the acyl group from acyl-ACP to proHlyA (*12*). The reaction kinetics are consistent with a ping-pong mechanism. Thus, the acyl transfer consists of two partial reactions. The first partial reaction has been shown, and the acyl-HlyC intermediate has been isolated and characterized (*19*−*22*). As specified above, internal acylation of proHlyA by HlyC occurs on two precise lysine residues, but what constitutes an acylation site is not clear. The amino acid sequences flanking the two sites are not homologous except that each has a glycine residue immediately preceding the lysine which is acylated (Figure 1); there are, however, numerous GK sequences throughout proHlyA that are not acylation sites. There is no persuasive indication of what determines the substrate specificity of the highly specific acylation of proHlyA. Keeping in mind the possibility of interaction between the two acylation sites, we have examined the effects of altering the acylation substrates on the efficacies of acylation by creating substantial deletions of proHlyA, separating the acylation sites into two different peptides, and carrying out site-directed mutation analyses of the acylation sites.

EXPERIMENTAL PROCEDURES

Materials and Services. [1-^{14}C]Myristate was from New England Nuclear. Peptides, TOX1 and TOX2 (>95% pure) and TOX3 and TOX4 (unpurified), from Sigma-Genosys were dissolved in 25 mM Hepes (pH 8.0). Peptide TOX5 (~70% pure) from NewEngland Peptide was dissolved in 25 mM Hepes (pH 6.5). *Eco*RV, *Dpn*I, and Deep Vent DNA polymerase were from New England Biolabs. *Pfu Turbo* DNA polymerase was from Stratagene. 3-(1-Pyridinio)-1-propanesulfonate was from Fluka. All chemicals were reagent grade. Urea-containing buffers were freshly prepared and kept at −20 °C. Novagen was the source of alkaline phosphatase-conjugated S-peptide and pET plasmids. Millipore was the source of YM-10 microcons. Ni−NTA spin columns were from Qiagen and were used according to instructions. Computational comparisons of RTX A proteins were performed at the Swiss Institute of Bioinformatics using the BLAST network service.

Bacterial Strains, Growth Media, and DNA. E. coli strains were as follows: BL21(DE3)pLysS from Novagen, DH5α-PRO from Clontech, and XL-2 Blue from Stratagene. Cells were grown in Luria broth except for the expression of HlyC. HlyC expression cells were grown in M9 minimal medium, induced with 1 mM IPTG at an A_{600} of 0.6, and harvested after 3.5 h. Oligonucleotides used for subcloning fragments of the *hlyA* gene or site-directed mutagenesis of *hlyA*, *frag A*, and *frag B* genes were from Integrated DNA Technologies and are given in Table 1. DNA between bp 1414 and 1983 of the pHly152 *hly* determinant (*23*) encoding a portion of the *hlyA* gene designated as frag B was subcloned from pTXA1 (*12*) using PCR with Deep Vent DNA polymerase. The purified amplified DNA was blunt-end-ligated into the *Eco*RV site of pET-30(b) which encoded an N-terminal His_6-S-tag fused with the fragment of proHlyA, resulting in pTXAt2. This plasmid was transformed into BL21(DE3)-pLysS cells for expression. To generate frag C, DNA between bp 1740 and 2340 of the pHly152 *hly* determinant encoding a portion of the *hlyA* gene was subcloned from pTXA1 via PCR using Deep Vent DNA polymerase. It was ligated into the *Eco*RV site of the pET30b vector. The plasmid encoding frag C was called pTXAt3.

For insertion into a new vector, the *HlyA* gene was amplified with PCR from pTXA1 using primers containing *Kpn*I and *Xba*I sites. The purified DNA was ligated into the corresponding endonuclease sites on the pPROTet·E133 vector from Clontech Laboratories, Inc., resulting in pTXA2 which was then transformed into DH5αPRO cells for expression.

Table 1: Sequences of Primers Used To Construct ProHlyA and Frag A Subclones, Frag B, Frag C, and Site-Directed Mutations of ProHlyA, Frag A, and Frag B

name[a]	sequence (from 5′ to 3′)
proHlyA K690A 5′	GAGGTTTCAGTCGGAGCAAGAACTGAAAAAACGC
proHlyA K690A 3′	GCGTTTTTTCAGTTCTTGCTCCGACTGAAACCTC
proHlyA K564A 5′	AGGAGGCAGTCCGGAGCATATGAATATATTACCGAG
proHlyA K564A 3′	CTCGGTAATATATTCATATGCTCCGGACTGCCTCCT
proHlyA K690C 5′	GAGGTTTCAGTCGGATGCAGAACTGAAAAAACGC
proHlyA K690C 3′	GCGTTTTTTCAGTTCTGCATCCGACTGAAACCTC
proHlyA K690L 5′	GGAGGTTTCAGTCGGACTGAGAACTGAAAAAACGC
proHlyA K690L 3′	GCGTTTTTTCAGTTCTCAGTCCGACTGAAACCTCC
proHlyA K564C 5′	AGGAGGCAGTCCGGATGCTATGAATATATTACCGAG
proHlyA K564C 3′	CTCGGTAATATATTCATAGCATCCGGACTGCCTCCT
proHlyA K564R 5′	AGGAGGCAGTCCGGACGTTATGAATATATTACCGAG
proHlyA K564R 3′	CTCGGTAATATATTCATAACGTCCGGACTGCCTCCT
frag B 5′	CTCAGTCCTCATTACCCAGCAACATTG
frag B 3′	CTACGCTTCGGTTGCTTTTGTGCCATC
frag C 5′	GGTGAAGGGGGTTCATTACAAG
frag C 3′	CTAATCACCGCCATAGAGCTGGTCATCTC
pTXA2 5′	GGGGTACCCATGACAACAATAACCACTGCAC
pTXA2 3′	GCCTCTAGATTATGCTGATGTGGTCAGGG

[a] Letters are one-letter amino acid abbreviations. The first 12 primers were used for site-directed mutagenesis of proHlyA or its fragments; the proHlyA primary structure designations are used for their description. The primers were used with the following templates for site-directed mutation or for subcloning the protein into plasmids: pTXA2 for proHlyA, pTXAt1 for frag A, and pTXAt2 for frag B. Where site-directed mutations were made in proHlyA or one of its fragments, the same primers were used, and the mutation site was described for the proHlyA site amino acid sequence.

Site-Directed Mutagenesis. Site-directed mutations were generated by the round circle PCR method described in the QuikChange site-directed mutagenesis kit protocol (Stratagene) using pTXA2, pTXAt1, or pTXAt2 plasmid as the reaction template (*21*). The rationale involved whole-plasmid PCR amplification using the mutagenic oligonucleotides shown in Table 1, one 5′ and one 3′ primer for each mutation. Residual native plasmid was digested with the *dam* methylation-specific restriction endonuclease *Dpn*I, and the PCR product containing the mutation was transformed into XL2-Blue cells for efficient cloning of nonmethylated DNA. Mutation of DNA was confirmed by DNA sequence analysis (*24*) at the Molecular Genetics Facility at the University of Georgia (Athens, GA). Plasmids containing mutant HlyA, frag A, or frag B inserts were designated pTXA, pTXAt1, or pTXAt2, respectively, along with a description of the mutation. The pTXAt1 and pTXAt2 vectors containing mutant genes were transformed into BL21(DE3)pLysS cells for expression. The pTXA vectors were transformed into DH5αPRO.

Expression of Proteins. Proteins were handled at 4 °C unless noted otherwise. ACPSH and [1-^{14}C]myristoyl-ACP were obtained as described by Trent and colleagues (*12*). Myristoyl-ACP was purified and evaluated as described previously (*25*) and stored in aliquots at −80 °C.

HlyC expressed as a His_6-S-tag fusion protein from pTXC2 described previously (*21*) was employed for kinetics. In experiments where peptides were used in the reaction, the HlyC that was used was expressed as an S-tag fusion protein encoded by pTXC1 (*12*). HlyC fusion proteins were purified from inclusion bodies (∼85−95% pure) as described previously (*20*).

ProHlyA was hyperexpressed from pTXA2 during 3 h following induction with 100 ng/mL anhydrotetracycline. Cells were harvested and stored, and HlyA was extracted from washed inclusion bodies as described by Trent and colleagues (*12*). From 500 mL of culture, 15 mg of 90% pure proHlyA was obtained.

N-Terminal His_6-S-tag fusion frag A, N-terminal His_6-S-tag fusion frag B, and N-terminal His_6-S-tag fusion frag C were hyperexpressed from cells grown as described previously for frag A expression (*20*), and the frag A was ∼92% pure. Following induction and harvest of a 500 mL culture and storage of the cell pellet at −20 °C, frag B or frag C was isolated from inclusion bodies using the procedure described for fragA (*20*).

Protein Determination. The amount of protein was measured as described by Bradford (*26*).

Gel Electrophoresis, Western Blotting, and Image Analysis. The purity of each protein that was used was assessed by densitometry following SDS−PAGE according to the method of Laemmli (*27*). Coomassie-stained gels were scanned using a Hewlet-Packard ScanJet 5200C scanner and analyzed with Un-Scan-It software by Silk Scientific. Western blotting onto a PVDF membrane (Bio-Rad) was done using a Bio-Rad Semi-Dry electrophoretic transfer cell according to the manufacturer's instructions. For imaging of ^{14}C-labeled proteins on Western blots, blots were placed in a BAS-MS 2025 Fujifilm imaging plate cassette and then analyzed in a Fujifilm FLA-5000 Science Imaging System equipped with Image Gauge version 3.46 and L Process version 1.96.

Assessment of Myristoyl-HlyC Formation. [1-^{14}C]Myristoyl-HlyC formation was assessed as described previously (*19*). In the experiments reported here, the HlyC concentration was 6 μM and that of [1-^{14}C]myristoyl-ACP was 1 μM. When TOX1 was used, it was added (500 μM) to the reaction mixture prior to the addition of [1-^{14}C]myristoyl-ACP.

Measurement of Enzyme Activity. The rate at which HlyC catalyzed acyl transfer from [1-^{14}C]myristoyl-ACP to proHlyA or one of its fragments (frag A, frag B, or frag C) was measured as previously described (*12*). Previously unthawed aliquots of protein acylation substrate and HlyC were used for each set of assays. Reactions were initiated by the addition of [1-^{14}C]myristoyl-ACP. Initial velocity kinetic data were analyzed by fitting eq 1 directly in the hyperbolic form

with an unweighted nonlinear regression analysis as described by Wilkinson (*28*) using Hyper (Emmet-Drury Software)

$$v = \frac{V_{max}[S]}{[S] + K_m} \quad (1)$$

where V_{max} is the maximal velocity and K_m the Michaelis constant for the varied substrate S. These analyses yielded the reported kinetic parameters. The first-order rate constant (also called the proportionality constant) for the reaction under defined conditions for a specified variable substrate was given by the equation "*k*" $\approx V_{max}^{app}/K_m^{app}$ (*29*). Data were also examined using several linear forms using a computer program described previously (*30*). Agreement among all methods was required for the acceptance of data (*12*). Data were plotted using Michaelis−Menten nonlinear regression analyses and linear regression analyses in GraphPad Prism version 4.

RESULTS

Characteristics of Subcloned Fragments of ProHlyA. A common element of many RTX proteins is the presence of one or two internal acylation sites. One hundred twenty-six amino acid residues separate the two sites in proHlyA, and a similar interval between acylation sites is found in other RTX toxins possessing two putative acylation sites. To examine the biochemistry of internal acylation of proHlyA, fragments of proHlyA were made. The 39.5 kDa frag A, which encompasses amino acid residues Ser472−Asp780 of proHlyA, includes both of the acylation sites shown in the structural representation in Figure 1, preserved as Lys140 and Lys266 of frag A (*20*). The relatively hydrophobic portion of proHlyA near the N-terminus (Figure 1) and the majority of the Ca^{2+} binding repeats were eliminated in constructing frag A. Frag A was subcloned and expressed as two smaller pepetides each fused with a His_6-S-tag, and each contained one of the two acylation sites present in proHlyA. Frag B (26.47 kDa), encompassing proHlyA residues Ser472−Ala661, contained the proHlyA Lys564 acylation site at Lys140. Frag C (27.03 kDa), encompassing proHlyA residues Val581−Asp780, contained the other acylation site, Lys690 of proHlyA, at Lys157. Frag B and frag C containing the fused N-terminal His_6-S-tags were hyperexpressed in good yield as fairly pure proteins (Figure 2A,B). Typical protein yields from 500 mL of culture were 11 mg for frag B (84% pure) and 26 mg for frag C (97% pure).

The fragments of proHlyA, frag A−frag C, were tested for their capacities to serve as in vitro substrates for internal protein acylation catalyzed by HlyC. Their substrate capabilities were verified by the transfer of radiolabeled myristate from [1-^{14}C]myristoyl-ACP to each of the subcloned fragments of proHlyA shown on the phosphoimage of the Western-blotted SDS−PAGE separation of the components of reaction mixtures containing acyl acceptors frag A, frag B, and frag C, respectively, in Figure 3 (first three lanes). The efficacies of the fragments as substrates for internal protein acylation were compared to that of proHlyA (Table 2). Frag A and frag B at 86 and 92% of proHlyA "*k*" approximated proHlyA as substrates for internal acylation,

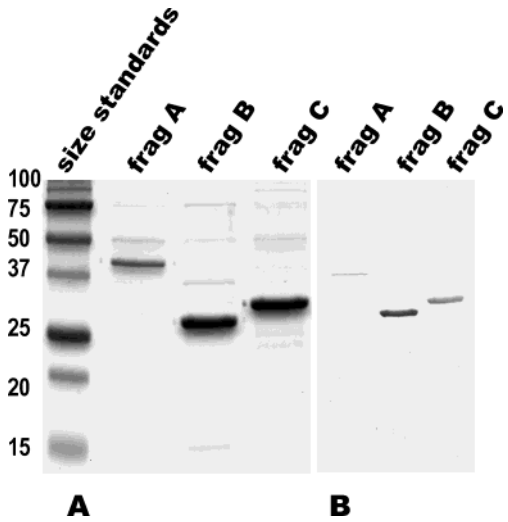

FIGURE 2: Expression and purification of His_6-S-tag fusion proteins frag A−frag C. An SDS−15% PAGE gel stained with Coomassie Blue (A) and its Western blot probed with the *S*-protein−alkaline phosphatase conjugate (B) show protein and S-tag correlations. Bio-Rad Precision Plus protein standards were used. Two micrograms of protein was loaded in each lane in panel A, and 2 μg was loaded in each lane in panel B. Units of sizing standards are kilodaltons.

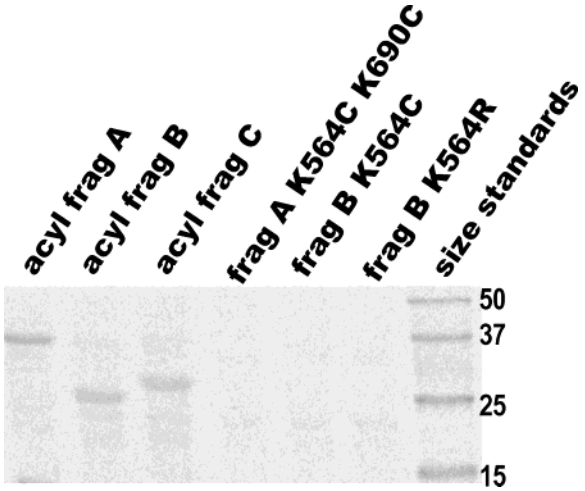

FIGURE 3: Phosphoimage of attempts to acylate wild-type and mutant frags using 2 μM acylation substrate, 1 μM HlyC, and 1 μM [1-^{14}C]myristoyl-ACP. The acylation reaction was carried out as described previously (*12*). After the reaction, proteins were separated via SDS−15% PAGE as described previously (*20*), blotted, and subjected to phosphoimage analysis as described in Experimental Procedures. The radioactive sizing standards were from AmershamPharmacia, and units are kilodaltons.

while frag C, which contained the second acylation site equivalent to proHlyA K690, exhibited a rate that was 13% of that of proHlyA. Changes in catalytic efficiencies among the substrates stemmed from changes in V_{max}^{app} since K_m^{app} values were practically unchanged compared to that of the native substrate; this was most evident for frag C.

Effects of Mutation of Acylation Sites. The two acyl acceptor sites of the natural acyl acceptor proHlyA were separately characterized. Each was removed, one at a time, by site-directed mutation of lysine to alanine (Table 3). ProHlyA K690A with a "*k*" of 9.2 was a trifle more effective as an acyl acceptor than the wild type, whose "*k*" was 7.7 (Table 1). K_m^{app} was virtually unchanged, but V_{max}^{app} increased slightly to 120% of that of the wild type. The K564A mutation in wild-type proHlyA, however, resulted

Table 2: Acylation Kinetics of Different Acyl Group Acceptors[a]

acylation substrate	K_m^{app} (μM)	V_{max}^{app} (pmol)[b]	"*k*"[c]	% of the proHlyA rate
proHlyA	1.0 ± 0.14	7.7 ± 0.35	7.7	100
frag A	0.99 ± 0.17	6.6 ± 0.46	6.7	86
frag B	0.96 ± 0.15	6.8 ± 0.37	7.1	92
frag C	1.3 ± 0.23	1.4 ± 0.13	1.1	13

[a] The HlyC assay procedure is described in Experimental Procedures; reactions were initiated with [1-^{14}C]myristoyl-ACP. Methods for analyzing kinetic constants and computing the standard errors are given in Experimental Procedures, and the procedure for computing standard errors was that described by Wilkinson (*27*). [b] V_{max} is given in units of picomoles per minute of reaction per 0.7 μM HlyC with 1 μM [1-^{14}C]myristoyl-ACP in 0.1 M Hepes (pH 8.0) and 0.5 M urea. [c] "*k*" is the proportionality constant of the reaction under the defined conditions, an estimate of the first-order reaction rate.

Table 3: Acylation Kinetics of Acyl Acceptors Bearing Mutated Acylation Sites[a]

acyl acceptor mutation	corresponding wild-type proHlyA acylation site	K_m^{app} (μM)	V_{max}^{app} (pmol)[b]	"*k*"[c]
proHlyA K690A	K564	1.0 ± 0.09	9.2 ± 0.28	9.2
proHlyA K564A	K690	1.5 ± 0.29	1.0 ± 0.10	0.67
proHlyA K564A/K690A	none	0	0	inactive
frag A K690A	K564	1.2 ± 0.17	9.1 ± 0.48	7.6
frag A K690C	K564	1.9 ± 0.27	10.7 ± 0.60	5.6
frag A K690L	K564	1.7 ± 0.19	11.0 ± 0.05	6.5
frag A K564A/K690A	none	0	0	inactive
frag A K564C/K690A	none	0	0	inactive
frag A K564A	K690	0.86 ± 0.16	1.5 ± 0.12	1.7
frag B K564R	none	0	0	inactive
frag B K564C	none	0	0	inactive

[a] The HlyC assay and analysis of kinetic parameters are described in footnote a of Table 2. [b] V_{max} is defined in footnote b of Table 2. [c] "*k*" is defined in footnote c of Table 2.

in an abysmal acyl acceptor with a "*k*" of less than 1. Like frag C, the decreased activity of proHlyA K564A stemmed from a decreased V_{max}^{app}, while K_m^{app} was largely unchanged. The double mutant proHlyA K564A/K690A exhibited no activity as a substrate in the HlyC assay; thus, no other site in the molecule served as an acyl acceptor. Identical mutations in frag A had similar effects on the acyl acceptor capacities of the respective mutants. Again, the presence of the single functional acylation site corresponding to proHlyA K564 (Table 2) resulted in an acyl acceptor that was slightly more effective than wild-type frag A (Table 1), and when the single functional acylation site on frag A corresponded to proHlyA K690, the rate of catalysis was much reduced compared to that of wild-type frag A. Thus frag A, simpler, smaller, and more stable than proHlyA, was an equally suitable substrate for studying protein internal acylation since it demonstrated similar acylation efficacies.

As anticipated, mutation of both lysine acylation sites on frag A to alanines resulted in a protein that was not acylated by the acyltransferase HlyC. Another double mutant of frag A, K564C/K690A, was made to explore the possibility of the cysteine sulfhydryl group acting as an acyl acceptor in the assay, but there was no evidence of acylation of the mutant frag A when the enzyme was assayed or upon phosphoimage analysis of the reaction components separated by SDS−PAGE (Figure 3).

Table 4: Effects of Peptides Mimicking the Substrate Acylation Site on Internal Acylation of Proteins[a]

acylation substrate	peptide	% of 0 peptide acylation[b]		
		25 μM peptide	50 μM peptide	100 μM peptide
frag A	TOX1	50 ± 2	46 ± 7	37 ± 2
frag A	TOX2	92 ± 7	99 ± 1	113 ± 1
frag A	TOX5	70 ± 6	56 ± 6	ND
frag C	TOX1	ND	ND	44 ± 5

[a] Reaction conditions and assay procedures are described in footnote a of Table 2. In assays containing peptide, peptide was added with all reaction components prior to the start of the reaction with the addition of 1 μM [1-^{14}C]myristoyl-ACP. Reaction conditions were identical in all cases except for the acyl-acceptor concentration, which was 1 μM for profrag A and 1.3 μM for frag C; the HlyC concentration was 0.3 μM. The error estimates are standard deviations. The following numbers of points were averaged to obtain the data in the table: 6−10 assays for frag A with TOX2 and TOX5, 10 assays for frag A with TOX1, and 6 assays for frag C with TOX1. [b] For uninhibited assays in which frag A was the acyl acceptor, 12.6 ± 1.3 pmol of myristate per assay was transferred, and for assays in which frag C was the acyl acceptor, 2.03 ± 0.10 pmol of myristate per assay was transferred.

The acylation site lysine on frag B was mutated to cysteine and arginine. Neither of the frag B mutants served as an acyl substrate for HlyC as shown by the activity assay and phosphoimage analysis of the Western blot of reaction components separated by SDS−PAGE. This is evident in Figure 3 where lanes 5 and 6 show no radioactive acylation reaction product. Moreover, neither of the mutants inhibited the HlyC-catalyzed acylation of either frag A or frag B when present in a 4.2-fold excess (frag B K564R) or a 2.7-fold excess (frag B K564C) over wild-type frag B (data not shown), respectively.

Peptide Simulations of Acylation Sites. The lack of inhibition of acylation of wild-type substrates by mutants changed conservatively at only a single site, the acylation site, was unexpected. To overcome limitations on the concentrations of the mutated fragments that could be achieved in the assays, peptides mimicking the primary amino acid sequences surrounding proHlyA acylation sites Lys564 and Lys690 (Figure 1) were prepared. The residue corresponding to either Lys564 or Lys690 was changed to an arginine, so there was no unlikely chance of the peptide serving as an acyl substrate while the positive charge was preserved. Peptide TOX1 and TOX2 mimics of the proHlyA Lys564 region had sequences of TPGEEIRERRQSGRYEY-ITE and GEEIRERRQSGRYEYITELL, respectively, in which GR represents the wild-type site of acylation. A survey of the effects of the presence of the peptides in the assay of the acylation of frag A indicated that TOX1 at concentrations of ≥25 μM inhibited reaction at a frag A concentration of 1 μM (Table 4). Inhibition by TOX2 up to concentrations of 100 μM was not seen. Although the peptides mimicked the amino acid sequence surrounding the acylation site Lys564 of proHlyA, acylation of the site corresponding to Lys690 on frag C was inhibited to the same extent as that of frag A, where the most intense acylation activity was that of Lys564 (Table 4). The effects of varying concentrations of TOX1 on the kinetics of frag A acylation suggested that the inhibitory peptide was a competitive inhibitor of HlyC (Figure 4). The relationship between inhibitor concentration and K_m^{app} was linear (Figure 4 inset), suggesting a simple competitive inhibition with a K_i of ~21 μM. This was also the concentration of TOX1 that caused the slope of the $1/v$

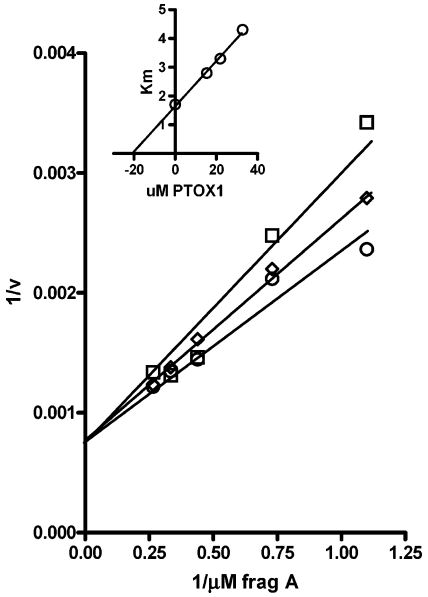

FIGURE 4: Lineweaver−Burk and secondary plots showing the competitive inhibition of frag A acylation by peptide TOX1. The assay procedure is cited in Experimental Procedures; the following substrates were present (in addition to the inhibitor): varying levels of frag A, 0.7 μM HlyC, and 1 μM [1-^{14}C]myristoyl-ACP. Frag A kinetic parameters were measured as described in the text either with no peptide (○) or in the presence of the following concentrations of TOX1: 15.28 (◇), 21.83 (□), and 32.75 μM (shown only in the inset). The inset is a replot of the K_m^{app} values determined in the presence of the different amounts of TOX1. The linear least-squares line had a slope of 0.079 ± 0.004 with an r^2 of 0.9957, and a K_i for TOX1 of 21 μM was estimated from the intercept.

versus 1/[S] plot to double, an independent estimate of the K_i, and another indicator of simple competitive inhibition (*31*).

The peptide mimic of the amino acid sequence surrounding proHlyA acylation site Lys690, TOX5, had the sequence QEVSVGRRTEKTQYRSYEFT, in which GR represents the wild-type site of acylation. TOX5 inhibited the acylation of frag A (Table 4), but it inhibited the reaction slightly less than TOX1 at comparable concentrations. The nature of TOX5 inhibition was not determined. Higher concentrations were incompatible with the assay procedure.

The following peptides mimicking the primary structure of the proHlyA Lys564 acylation site were constructed: HHHHGEEIRERRQSGKYEYI (TOX3) and HHHHHHT-PGEEIRERRQSGKYEYITE (TOX4). TOX3 resembled TOX2, and TOX4 was TOX1 with the N-terminal addition of six histidine residues. In both peptides, the Lys564 site of acylation was preserved, and they were used in the assay at relatively high concentrations (100 and 500 μM, respectively; 100 and 500 times greater, respectively, than the concentration of frag A when it was present) as potential sites of acylation. The peptides formed oils rather than precipitates in the presence of high concentrations of ammonium sulfate, so that procedure did not serve to separate them from [1-^{14}C]myristoyl-ACP which does not precipitate with ammonium sulfate. Using either Ni^{2+} chelating columns to capture the potential [1-^{14}C]myristoyl-peptide or, when that failed to demonstrate peptide acylation, Millipore YM-10 minicons to separate the relatively low-weight potential [1-^{14}C]myristoyl-peptide from the other larger reactants, there was no suggestion that the peptides served as acyl acceptors. Examination of TOX4 for potential inhibition by the procedures described above to assess TOX1, TOX2, and TOX5 did not reveal any tendency toward inhibition of frag A acylation when TOX4 was present in assays.

To further delineate the inhibitory effect of TOX1 on frag A acylation, the effect of TOX1 on the formation of [1-^{14}C]-myristoyl-HlyC, an intermediate formed in the first partial reaction of the two-step reaction (*18*) was examined. Using the same ratio of HlyC to TOX1 as that used in the third column of Table 4 where ~50% inhibition of frag A acylation was seen, there was no inhibition of acylation of HlyC to form myristoyl-HlyC (data not shown), the formation and stability of which have been reported previously (*12*, *18*, *19*).

DISCUSSION

Comparisons of the kinetics of acylation of proHlyA, frag A, and frag B show that all were comparable substrates for internal protein acylation. Frag C, which contains only the site equivalent to Lys690 of proHlyA, was a functional substrate but much less effective than those that contained the lysine acylation site equivalent to Lys564 of proHlyA. A fusion construct resembling frag C, a glutathione *S*-transferase−$HlyA_{S608-T725}$ fusion containing the second acylation site, K690, is acylated as judged by its response to a monoclonal antibody (*15*). The second acylation site Lys690 of proHlyA appears to be less conserved among RTX proteins than the site homologous to proHly Lys564 (*32*). In contrast to HlyA that is acylated at two sites with Lys564 being the more efficient site, *B. pertussis* RTX toxin CyA is activated by a single acylation at Lys983 that corresponds to the second *E. coli* proHlyA site, Lys690 (*33*).

Construction of fragments of proHlyA that served as substrates for internal protein acylation catalyzed by HlyC provided an opportunity for insight into the relationship of the two acylation sites. Mutations of acylation site lysines to alanine on frag A or proHlyA resulted in kinetics that resembled those seen when the acylation sites were located on separate molecules, i.e., frag A compared to frag B and frag C. When the data were grouped as Lineweaver−Burk plots, the kinetic relationship among the acylation sites either within a single structure or among the separate frag proteins resembled classical noncompetitive inhibition. Figure 5 shows the relationship among the kinetics of the acylation sites of frag A. Similar patterns were seen within the following sets: (1) the kinetics of frag A, frag B, and frag C and (2) the kinetics of the acylation sites of proHlyA and its mutations, singly, from lysine to alanine at each acylation site. There was essentially no change in K_m^{app} among the various substrates, wild-types, and acylation site mutants; rather, V_{max}^{app} changed (Table 3). In most instances of enzyme catalysis, substrate binding occurs faster than breakdown of the ES complex, so K_m^{app} is often an indication of substrate affinity (*29*), which was similar for both acylated sites. Within this scenario, the change in V_{max}^{app} perhaps arose from the $E\cdot_{690-acyl}S$ complex breaking down more slowly than the $E\cdot_{564-acyl}S$ complex, thus explaining the difference between the two sites, while the V_{max}^{app}, when both sites functioned, was the sum of the values for the two reactions (*34*). The maximum efficiency of the enzyme was seen when only the first acylation site, the equivalent of proHlyA K564,

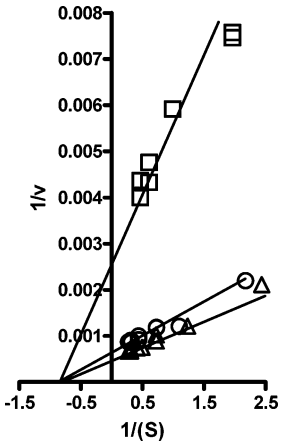

FIGURE 5: Lineweaver−Burk plot illustrating the site-directed mutation analysis of the kinetic relationship between the acylation sites in frag A. Kinetic parameters were measured under identical conditions as described in the text for frag A (○), frag A K690A (△), and frag A K564A (□).

was present; when both sites were present, the V_{max}^{app} was slightly lower. This describes a situation where the enzyme that was employed at the less efficient site was not available for catalysis at the more efficient site, a situation that manifested itself as less enzyme functioning within the system, a lower V_{max}^{app}. Such an interpretation was supported by the greatly decreased rate of catalysis observed with the second acylation site, the equivalent of proHlyA K690, as the sole substrate. The enzyme shared between two acylation sites was less efficient than the entire enzyme functioning at the more efficient site. This situation was, in essence, the simultaneous offering of two substrates, the two distinct acylation sites, in equal molar amounts to the enzyme. Under this circumstance, the ratio of the proportionality constants, "*k*", for the two substrates determines the ratio of the rates of the competing reactions when the substrates are both present (*35*). In frag A, the rate of acylation of the site equivalent to proHlyA K564 was 507% faster, 6.1 times faster, than the rate of acylation of the other acylation site, the equivalent of proHlyA K690. In a similar comparison between frag B and frag C, the rate of acylation of frag B was 546% faster, 6.5 times faster, than the rate of acylation of frag C. The relationships between the acylation sites were similar whether they were analyzed in the same molecule via site-directed mutation or analyzed in separate molecules.

Data presented here indicate that the two acylation sites in the *E. coli* hemolysin system functioned largely independently of one another in their interaction with HlyC; this agrees with observations from in vivo activation of hemolysin and studies of the hemolytic potential of bacterial growth supernatant medium (*36*). As mentioned earlier, *B. pertusis* CyaA is activated by a single acylation at Lys983 that corresponds to the *E. coli* HlyA Lys690 site, but in contrast to the seeming independence of *E. coli* hemolysin acylation sites, the biological activity of the monoacylated CyaA toxin, nevertheless, requires the integrity of Lys860, the lysine residue corresponding to the Lys564 site of acylation in HlyA, even though it is not normally acylated in CyaA (*33, 37*).

The lack of inhibition of HlyC by acylation site mutants of frag B, the wild type of which is an excellent substrate for acylation, was surprising. The amino acid sequence common to frag B and frag C between the acylation sites on frag A was also regarded as a potential inhibitor (Figure 1). The presence of this sequence in 2-fold excess of the acylation substrate, however, had no effect on activity (data not shown). In this vein, HlyA mutants with deletions of portions of the sequence separating the two acylation sites (Δ613−621 and Δ622−657) are not impaired in in vivo acylation (*36*). The possibility that HlyC binding occurred between the two acylation sites, thus accessing both acylation sites from a single binding site, is unlikely. In contrast, the reaction was inhibited by two peptides that mimicked the primary sequences surrounding either the Lys564 or Lys690 acylation sites, albeit slightly more effectively by the Lys564 mimic TOX1 whose inhibition was shown to be competitive. Interaction between HlyC, actually acyl-HlyC as shown above and explained in reaction 2 below, and the individual acylation sites is likely an integral part of the internal protein acylation reaction. Inhibition of acylation of frag C that contains only the Lys690 acylation site by the inhibitory peptide that mimicked the Lys564 acylation site was congruent with the supposition that acyl-HlyC interacted with each of the acylation sites, one at a time. According to the ping-pong reaction mechanism established for this reaction (*20*), the protein substrate to be acylated interacts with acyl-HlyC in the second partial reaction shown below (*19*).

1) acyl-ACP + HlyC ↔ [HlyC•acyl-ACP] ↔ acyl-HlyC + ACPSH

2) acyl-HlyC + proHlyA ↔ [proHlyA•acyl-HlyC] ↔ HlyA + HlyC

sum) acyl-ACP + proHlyA ↔ HlyA + ACPSH

Demonstration that TOX1 did not inhibit myristoyl-HlyC formation while it inhibited frag A and frag C acylations supports the assertion that inhibitory peptides exerted their effects by binding specifically to acyl-HlyC, not HlyC, and again verified the independence of the partial reactions (*19*). Acyl-HlyC interacted with one (TOX1) of the two 20-residue peptides that differed from the other only by the placement of two amino acid residues in the proHlyA sequence surrounding Lys564 which was replaced with an arginine; acyl-HlyC did not react with the other peptide (TOX2) under the same conditions. The TOX1 sequence was moved two residues toward the N-terminus of proHlyA compared to TOX2 (Figure 1). The C-terminal side of the acylation site possibly participated less in acylation site recognition by acyl-HlyC than the N-terminal side of the acylation site. On the N-terminal side, inclusion of either the proline residue or proline and threonine residues was crucial for interaction with acyl-HlyC. The parameters of the two peptides are quite similar; they are identically charged. The predictions of secondary structure using the Hierarchical Neural Network method (*38*) were, like their biological effects, quite different for the two peptides. TOX1 scored a more organized structure with 35% α-helix, 20% extended strand, and 45% random coil, while TOX2 exhibited 10% α-helix, 30% extended strand, and 60% random coil. The difference in biological activity possibly stemmed from structural differences in the two peptides, a reflection of the slight difference in the sequences.

A similarly sized peptide mimic of the sequence surrounding proHlyA Lys 690, TOX5, also inhibited the frag A acylation reaction slightly less effectively than TOX1. TOX5,

in contrast to TOX1 and TOX2, was basic and was estimated to have ~95% random coil structure. The amino acid sequences surrounding the two proHlyA acylation sites did not resemble one another, yet their K_m values were similar; in this sense, the qualitative similarity of inhibition by the two peptides, TOX1 and TOX5 mimicking each of the sites, is noteworthy. In contrast to the interaction of these peptides with the enzyme, peptides TOX3 and TOX4, up to 26 amino acids in length and mimicking the more favorable acylation substrate site, did not serve as acylation substrates, nor did TOX4 inhibit frag A acylation, suggesting impaired binding to the enzyme. Although the two acylation sites exhibited similar K_m values and similar mimetic peptide behaviors, the V_{max} values were substantially different. Perhaps the acylatability of potential substrates may also be anticipated to be variable in that binding and acylation are likely separate events.

RTX toxin acylation is the single event that entrains the pathologic events upon infection (*18*). The nature of the acyl groups that can be, as mentioned earlier for HlyA, quite varied (*14*) and their distribution between the acylation sites are suspected to be major determinants of the cellular specificities of RTX toxins (*38*). Thus, it is important to try to understand what in a protoxin constitutes an acylatable site and its proclivity for acylation. The substrate specificities of the acylation reactions are an integral part of understanding the pathologies of the various RTX toxins.

CONCLUSION

Different constructs of proHlyA served as internal protein acylation substrates. The two sites of acylation of proHlyA functioned independently of one another with HlyC; there did not appear to be a common HlyC binding site or processivity of the enzyme between the sites. The acylation substrate likely interacts directly with acyl-HlyC. Replacement of a lysine residue in the acyl acceptor sites with cysteine did not result in an acyl-protein. Internal protein acylation was inhibited by specific small peptides mimicking each acylation site primary structure; the acylation, however, of similar small peptides could not be shown.

REFERENCES

1. Melkonian, K. A., Ostermeyer, A., Chen, J. Z., Roth, M., and Brown, D. A. (1999) Role of lipid modifications in targeting proteins to detergent-resistant membrane rafts, *J. Biol. Chem. 274*, 3910−3917.
2. Arni, S., Keilbaugh, S. A., Ostermeyer, A., and Brown, D. A. (1998) Association of GAP-43 with detergent-resistant membranes requires two palmitoylated cysteine residues, *J. Biol. Chem. 273*, 28478−28485.
3. Farazi, T. A., Waksman, G., and Gordon, J. I. (2001) The biology and enzymology of protein *N*-myristoylation, *J. Biol. Chem. 276*, 39501.
4. Hedo, J. A., Collier, C., and Watkinson, A. (1987) Myristoyl and palmitoyl acylation of the insulin receptor, *J. Biol. Chem. 262*, 954−957.
5. James, G., and Olson, E. N. (1990) Fatty acylated proteins as components of intracellular signaling pathways, *Biochemistry 29*, 2624−2634.
6. Bhatnagar, R. S., and Gordon, J. I. (1997) Understanding covalent modifications of protein by lipids: Where cell biology and biophysics mingle, *Trends Cell Biol. 7*, 14−20.
7. Linder, M. E., and Deschenes, R. J. (2003) New insights into the mechanisms of protein palmitoylation, *Biochemistry 42*, 4311−4320.
8. Towler, D., and Glaser, L. (1986) Acylation of cellular proteins with endogenously synthesized fatty acids, *Biochemistry 25*, 878−884.
9. Nicaud, J. M., Mackman, N., Gray, L., and Holland, I. B. (1985) Characterization of HlyC and mechanism of activation and secretion of hemolysin from *E. coli* 2001, *FEBS Lett. 187*, 339−344.
10. Welch, R. A. (2001) RTX toxin structure and function: A story of numerous anomalies and few analogies in toxin biology, *Curr. Top. Microbiol. Immunol. 257*, 85−111.
11. Stanley, P., Packman, L., Koronakis, V., and Hughes, C. (1994) Fatty acylation of two internal lysine residues required for the toxin activity of *Escherichia coli* hemolysin, *Science 266*, 1992−1996.
12. Trent, M. S., Worsham, L., and Ernst-Fonberg, M. L. (1998) The biochemistry of hemolysin toxin activation: Characterization of HlyC, an internal protein acyltransferase, *Biochemistry 37*, 4644−4652.
13. Ludwig, A., Garcia, F., Bauer, S., Jarchau, T., Benz, R., Hoppe, J., and Goebel, W. (1996) Analysis of the in vivo activation of hemolysin (HlyA) from *Escherichia coli*, *J. Bacteriol. 178*, 5422−5430.
14. Lim, K. G., Walker, C. R. B., Guo, L., Pellett, S., Shabanowitz, J., Hunt, D. F., Hewlett, E. L., Ludwig, A., Goebel, W., Welch, R. A., and Hackett, M. (2000) *Escherichia coli* α-hemolysin (HlyA) is heterogeneously acylated in vivo with 14-, 15-, and 17-carbon fatty acids, *J. Biol. Chem. 275*, 36698−36702.
15. Pellett, S., and Welch, R. A. (1996) *Escherichia coli* hemolysin mutants with altered target cell specificity, *Infect. Immun. 64*, 3081−3087.
16. Bauer, M. E., and Welch, R. A. (1996) Association of RTX toxins with erythrocytes, *Infect. Immun. 64*, 4665−4672.
17. Moayeri, M., and Welch, R. A. (1997) Prelytic and lytic conformations of erythrocyte-associated *Escherichia coli* hemolysin, *Infect. Immun. 65*, 2233−2239.
18. Uhlen, P., Laestadius, A., Jahnukainen, T., Söderblom, T., Bäckhed, F., Celsi, G., Brismar, H., Normark, S., Aperia, A., and Richter-Dahlfors, A. (2000) α-Haemolysin of uropathogenic *E. coli* induces Ca^{2+} oscillations in renal epithelial cells, *Nature 405*, 694−697.
19. Trent, M. S., Worsham, L., and Ernst-Fonberg, M. L. (1999) HlyC, the internal protein acyltransferase that activates hemolysin toxin: Roles of various conserved residues in enzymatic activity as probed by site-directed mutagenesis, *Biochemistry 38*, 9541−9548.
20. Worsham, L., Trent, M. S., Earls, L., Jolly, C., and Ernst-Fonberg, M. L. (2001) Insights into the catalytic mechanism of HlyC, the internal protein acyltransferase that activates *Escherichia coli* hemolysin toxin, *Biochemistry 40*, 13607−13616.
21. Trent, M. S., Worsham, L., and Ernst-Fonberg, M. L. (1999) HlyC, the internal protein acyltransferase that activates hemolysin toxin: Role of conserved histidine, serine, and cysteine residues in enzymatic activity as probed by chemical modification and site-directed mutagenesis, *Biochemistry 38*, 3433−3439.
22. Trent, M. S., Worsham, L., and Ernst-Fonberg, M. L. (1999) HlyC, the internal protein acyltransferase that activates hemolysin toxin: the role of conserved tyrosine and arginine residues in enzymatic activity as probed by chemical modification and site-directed mutagenesis, *Biochemistry 38*, 8831−8838.
23. Hess, J., Wels, W., Vogel, M., and Goebel, W. (1986) Nucleotide sequence of a plasmid-encoded hemolysin determinant and its comparison with a corresponding chromosomal hemolysin sequence, *FEMS Microbiol. Lett. 34*, 1−11.
24. Sanger, F., Nicklen, S., and Coulson, A. R. (1977) DNA sequencing with chain terminating inhibitors, *Proc. Natl. Acad. Sci. U.S.A. 74*, 5463−5467.
25. Worsham, L., Williams, S., and Ernst-Fonberg, M. L. (1993) Early catalytic steps of *Euglena gracilis* choroplast type II fatty acid synthase, *Biochim. Biophys. Acta 1170*, 62−71.
26. Bradford, M. M. (1976) A rapid and sensitive method for the quantitation of microgram quantities of protein utilizing the principle of protein-dye binding, *Anal. Biochem. 72*, 748−754.
27. Laemmli, V. (1970) Cleavage of structural proteins during the assembly of the head of bacteriophage T4, *Nature 227*, 680−685.
28. Wilkinson, G. N. (1961) Statistical estimations in enzyme kinetics, *Biochem. J. 80*, 324−332.
29. Marangoni, A. G. (2003) *Enzyme Kinetics: A Modern Approach*, pp 48−51, John Wiley & Sons, Hoboken, NJ.

30. Walker, T. A., Jonak, Z. L., Worsham, L. M. S., and Ernst-Fonberg, M. L. (1981) Kinetic studies of the fatty acid synthetase multienzyme complex from *Euglena gracilis* variety *bacillaris*, *Biochem. J. 199*, 383−392.
31. Segel, I. H. (1975) *Enzyme Kinetics: Behavior and Analysis of Rapid Equilibrium and Steady State Enzyme Systems*, pp 100−111, John Wiley & Sons, New York.
32. Altschul, S. F., Madden, T. L., Schäffer, A. A., Zhang, J., Zhang, Z., Miller, W., and Lipman, D. J. (1997) Gapped BLAST and PSI-BLAST: A new generation of protein database search programs, *Nucleic Acids Res. 25*, 3389−3402.
33. Basar, T., Havlíček, V., Bezušková, S., Halada, P., Hackett, M., and Šebo, P. (1999) The conserved lysine 860 in the additional fatty-acylation site of *Bordetella pertussis* adenylate cyclase is crucial for toxin function independently of its acylation status, *J. Biol. Chem. 274*, 10777−10783.
34. Dixon, M., and Webb, E. C. (1970) *Enzymes*, 3rd ed., p 337, Academic Press, New York.
35. Cornish-Bowden, A. (1979) *Fundamentals of Enzyme Kinetics*, pp 84−85, Butterworths, London.
36. Ludwig, A., Garcia, F., Bauer, S., Jarchau, T., Benz, R., Hoppe, J., and Goebel, W. (1996) Analysis of the in vivo activation of hemolysin (HlyA) from *Escherichia coli*, *J. Bacteriol. 178*, 5422−5430.
37. Basar, T., Havlíček, V., Bezoušková, S., Hackett, E. L., and Šebo, P. (2001) Acylation of lysine 983 is sufficient for toxin activity of *Bordetella pertussis* adenylate cyclase, *J. Biol. Chem. 276*, 348−354.
38. Combet, C., Blanchet, C., Geourjon, C., and Deléage, G. (2000) NPS@: Network protein sequence analysis, *Trends Biochem. Sci. 25*, 147−150.
39. Westrop, G., Hormozi, K., DA Costa, N., Parton, R., and Coote, J. (1997) Structure−function studies of the adenylate cyclase toxin of *Bordetella pertussis* and the leukotoxin of *Pasturella haemolytica* by heterologous C protein activation and construction of hybrid proteins, *J. Bacteriol. 179*, 871−879.

BI035919K